

1 **Effects of climate change on the design of subsurface drainage systems in coastal aquifers in**
2 **arid/semi-arid regions: Case study of the Nile delta**

3 *Ismail Abd-Elaty¹, Gehan.A.H.Sallam², Salvatore Straface³ and Andrea Scozzari⁴*

4
5 ¹Department of Water and Water Structures Engineering, Faculty of Engineering, Zagazig University, Zagazig 44519,
6 Egypt.

7 ²Drainage Research Institute (DRI), National Water Research Center (NWRC), Cairo, Egypt

8 ³ Department of Environmental and Chemical Engineering, University of Calabria, Ponte P. Bucci, 87036 Rende, Italy

9 ⁴CNR Institute of Information Science and Technologies (CNR-ISTI), Via Moruzzi 1, 56024 Pisa, Italy,
10 Email: a.scozzari@isti.cnr.it

11 **Keywords:** sea level rise, coastal aquifer, climate change, subsurface draining systems, seawater intrusion

12 **ABSTRACT:**

13 The influence of climate change on the availability and quality of both surface- and ground-water resources
14 is well recognized nowadays. In particular, the mitigation of saline water intrusion mechanisms in coastal
15 aquifers is a recurrent environmental issue. In the case of the Nile delta, the presence of sea level rise and
16 the perspective of other human-induced stressors, such as the next operation of the Grand Ethiopian
17 Renaissance Dam, are threats to be taken into account for guaranteeing resilient agricultural practices within
18 the future possible scenarios. Subsurface drainage offers a practical solution to the problem of upward
19 artesian water movement and the simultaneous downward flow of excess irrigation water, to mitigate the
20 salinization in the root zone. Subsurface draining systems can contribute to mitigate the vulnerability to
21 climate change and to the increased anthropic pressure insofar they are able to receive the incremented flow
22 rate due to the foreseen scenarios of sea level rise, recharge and subsidence. This paper introduces a rational
23 design of subsurface drainage systems in coastal aquifers, taking into account the increment of flow in the
24 draining pipes due to future possible conditions of sea level rise, artificial recharge and subsidence within
25 time horizons that are compatible with the expected lifespan of a buried drainage system. The approach
26 proposed in this paper is characterised by the assessment of the incremental flow through the drains as a
27 function of various possible scenarios at different time horizons. Our calculations show that the impact on
28 the discharge into the existing subsurface drainage system under the new foreseen conditions is anything
29 but negligible. Thus, future climate-related scenarios deeply impact the design of such hydraulic structures,
30 and must be taken into account in the frame of the next water management strategies for safeguarding
31 agricultural activities in the Nile delta and in similar coastal contexts.

1 Introduction

Climate change is a global phenomenon; however it's very variable on a geographical basis. It is defined as an imbalance in the usual climatic conditions such as heat, wind and rainfall patterns that characterize each region on earth. A number of phenomena is addressed to produce the sea level rise (SLR), and its acceleration that is currently observed, such as the thermal expansion of the oceans and seas, the melting of glaciers and ice caps including Greenland, and Antarctic ice sheets melting. According to the Intergovernmental Panel on Climate Change (IPCC, [2013](#)), in year 2100 about 95% of the coastal areas in the world will be considerably affected by SLR, hence increasing the risk of inundation in internal land and salt water intrusion (SWI) in coastal aquifers (Agren and Svensson, 2017). Shaltout et al. (2015) indicated SLR effects in the Nile delta in terms of ongoing submergence. According to Sestini (1989) and IPCC (2008), Egypt is considered among the most vulnerable countries to the threat taken by SLR.

Recent measurements by both ground based and satellite observations also indicate an acceleration in the rates of SLR (Legeais et al., 2018). El Raey (2010) studied both environmental and socio-economical risks in the coastal zone of the Nile delta connected with climate change, also placing attention to SLR and subsidence. The IPCC in its 5th report (IPCC, 2013) predicts global SLR figures from 18 to 59 cm in the next 100 years. For what regards Egypt, such conditions would lead to the submergence of the low lying coastal zones and some parts of the Nile Delta adjacent to the [northern](#) coast. In addition to surface water issues, a particularly challenging aspect is the mitigation of saline water intrusion mechanisms (SWI) in groundwater, in the presence of sea level rise and with the perspective of other human-induced stressors, such as the next operation of the [Grand Ethiopian Renaissance Dam \(GERD\)](#), the overpopulation in the Nile delta and Nile valley, and the various forms of desertification processes currently observed (Aboel Ghar et al, 2004). The risk of increased salinization deeply impacts agricultural practices and must also be taken into account for the management of reclaimed lands.

The Nile delta aquifer is a Quaternary aquifer mainly composed of a Holocene clay cap layer and a series of Pleistocene layers (deepest confined aquifer). The Holocene clay cap acts as an aquitard in its southern part, with an average thickness between 5 and 25 m, while in the northern parts it acts as an aquiclude and its thickness is larger than 50 m (Said, 1962, 1981; Serag EI-Din, 1989). The Pleistocene layers consist of coarse-grained Quartzitic sands and gravels alternated by lenses of clay. Its thickness gradually increases

60 [toward the sea, being about 200 m in the South and sometimes exceeding 950 m in the North \(El-Fayoumi,](#)
61 [1987; Said, 1993\).](#)

62 Both the risk of submergence and SWI are exacerbated by subsidence (Wöppelmann et al, 2013). [Several](#)
63 [mechanisms could be brought as cause of subsidence: the sediment loading and isostatic displacement, or](#)
64 [the failure, faulting, and flow of under-consolidated sediments, the anthropogenic or tectonics factors and](#)
65 [the sediment compaction. Analysing the scales, the patterns and the velocities observed across the northern](#)
66 [Nile Delta, the sediment compaction is the only subsidence mechanism consistent with them. Rapid](#)
67 [compaction rates have been recorded in the meter increment below the top 1.0 to 2.0 meters of sediment on](#)
68 [the Nile Delta. These rates appear to decrease to around 5.0 to 6.0 meters in an irregular fashion and then](#)
69 [continue to decrease more regularly to the base of the Holocene section \(Stanley and Corwin, 2012\). Much](#)
70 [of the subsidence measured by previous studies occurs in conjunction with known Holocene sediment](#)
71 [deposits. Therefore, subsidence patterns do appear to correlate with thick Holocene sediment](#)
72 [accumulations, but also appear to be heavily influenced by young sediment deposits of less than 3500 years](#)
73 [old due to rapid compaction within the first few meters \(Fugate, 2014\).](#)

74 [Subsidence](#) exhibits variable rates across the Nile delta (Becker and Sultan, 2009; Fugate, 2014), often
75 higher than SLR. In particular, it is expected that vertical land motion has a relevant impact on the
76 assessment of future scenarios and the relating time horizon, regarding the risks of both submergence and
77 salt water intrusion. In particular, the combination of SLR and subsidence has an impact on the design of
78 drainage systems, especially in view of an acceleration of both phenomena.

79 Laeven (1991) showed that the saline water of the Mediterranean Sea intrudes into the Nile aquifer at depths
80 in the range from 175 to 225 m, in the deepest confined aquifer. Moreover, Sakr et al. (2004) analyzed the
81 historical records from 1960 to 2000 and demonstrated the sensitivity of groundwater salinity with respect
82 to the Nile flow and abstraction rates. Authors concluded that the reduction in the Nile flow and the
83 extensive abstraction from the aquifer lead to an increase in groundwater salinity. The effect of Nile flow
84 reduction, which is expected when the GERD will enter into operation (Abd-Elhamid et al., 2018),
85 combined with the increased pumping of groundwater and the current trend of sea level rise is expected to

86 affect seawater intrusion mechanisms in the Nile Delta in a dramatic way, requiring the urgent identification
87 and design of possible counter-measures.

88 Several studies were carried out on the Nile delta confined aquifer to investigate the possible impact of
89 SLR, including Sherif and Al-Rashed (2001), Sherif et al. (2012), Sefelnasr and Sherif (2014), Abd-Elaty
90 et al. (2014) and Abd-Elhamid et al. (2016). These studies indicated that SLR has a negative impact on
91 saltwater intrusion, predicting a sure threat to a large quantity of freshwater. An alternative strategy to
92 mitigate the SLR effects is the artificial recharge (AR). In the coastal aquifer it reduces the seawater
93 intrusion growing the fresh water pressure in the aquifer. AR requires an increase of alternative water
94 supplies, such as desalination plants and water reuse from one side and aquifer recharge systems on the
95 other side (Abd-Elhamid and Abd-Elaty, 2017).

96 Drainage is an essential practice in agricultural irrigated lands for preventing water-logging and salinization
97 (Abd-Elaty et al., 2010). When the conditions in an area are such that an upward seepage from an underlying
98 aquifer occurs, the risks of water logging and salinity are more serious. Such conditions may prevail in
99 some areas of the Nile delta. Especially the northern coast is expected to be negatively impacted by both
100 SLR and subsidence in the future. Subsurface drainage offers a possible practical solution for avoiding the
101 salinization of the ground in the root zone, in the presence of upward artesian water movement with a
102 simultaneous downward flow of excess irrigation water.

103 The design objective of the drains is to keep the water table within specified limits, determining a flow of
104 water through the soil to the drains. Bazaraa et al. (1986) studied the artesian and anisotropic effects on
105 drain spacing. Subsurface drainage systems installed in a soil overlying an artesian aquifer should be
106 designed to handle both the upward artesian water flow and the downward seepage flow due to irrigation
107 and rainfall. Proper drain spacing and sizing depends on several parameters, and it is known that drains
108 subject to artesian conditions require a narrower spacing with respect to the simplest condition characterized
109 by downward seepage only.

110 In 2011, Kalantari studied the impact of climate change on drainage systems. The study concluded that
111 hydrological models are fundamental tools to assess the discharge dynamics, and the expected changes due
112 to climate factors. Deelstra (2015) indicated that drainage construction is often carried out based on existing

113 practice and experience. Today, this might not be suitable under conditions of climate change, anthropic
114 pressure and increased extreme events. Therefore, factors of influence on the design of drainage systems
115 should be known and taken into account. A deep understanding of the interaction between climate,
116 geological setting, land use, watershed hydrology and groundwater flow is a necessary prerequisite for the
117 design of a draining system characterized by a long-enough service time horizon.

118 The design improvement of drainage systems according to new perspective scenarios characterized also the
119 recent literature related to the North American region. In 2017, Pease et al. used the DRAINMOD
120 hydrologic model to simulate the expected climate change effects on subsurface drainage and the
121 performance of controlled drainage in the western Lake Erie Basin (US), where the climate change is
122 expected to increase both annual rainfall and temperatures. The study indicated that the development of
123 strategies to mitigate the impact of these changes is important for ensuring agricultural resiliency to the
124 future climate. British Columbia (Canada) Agriculture & Food Climate Action Initiative (2013) reported
125 that, in the countries where subsurface drainage is necessary, a proper design of drainage systems must take
126 into account the mitigation of risks related with the climate change.

127 The adaptation of drainage systems design to climate change varies greatly depending on local conditions,
128 in Egypt most of the previous studies did not take into account the effect of climate change on subsurface
129 drainage design, neither the effect of subsidence was considered. This paper represents a first building block
130 for the proper design of subsurface drainage (SD) systems in the Nile delta and in coastal aquifers in general,
131 in the presence of multiple climate-related forcing parameters. In particular, attention is focused on SLR,
132 subsidence, and on the artificial subsurface recharge that is hypothesized in order to reduce the aquifer
133 salinity.

134 This paper introduces a rational design of subsurface drainage systems in coastal aquifers, by estimating
135 the flow in the draining pipes and its possible increment due to the foreseen scenarios of SLR, recharge and
136 subsidence. A novel approach proposed in this paper consists in the assessment of the incremental flow
137 through the drains as a function of various possible scenarios. The next sections will illustrate the
138 assumptions made and the methods used to build the scenarios, and the evaluation of the expected impact
139 on the design of subsurface drainage systems.

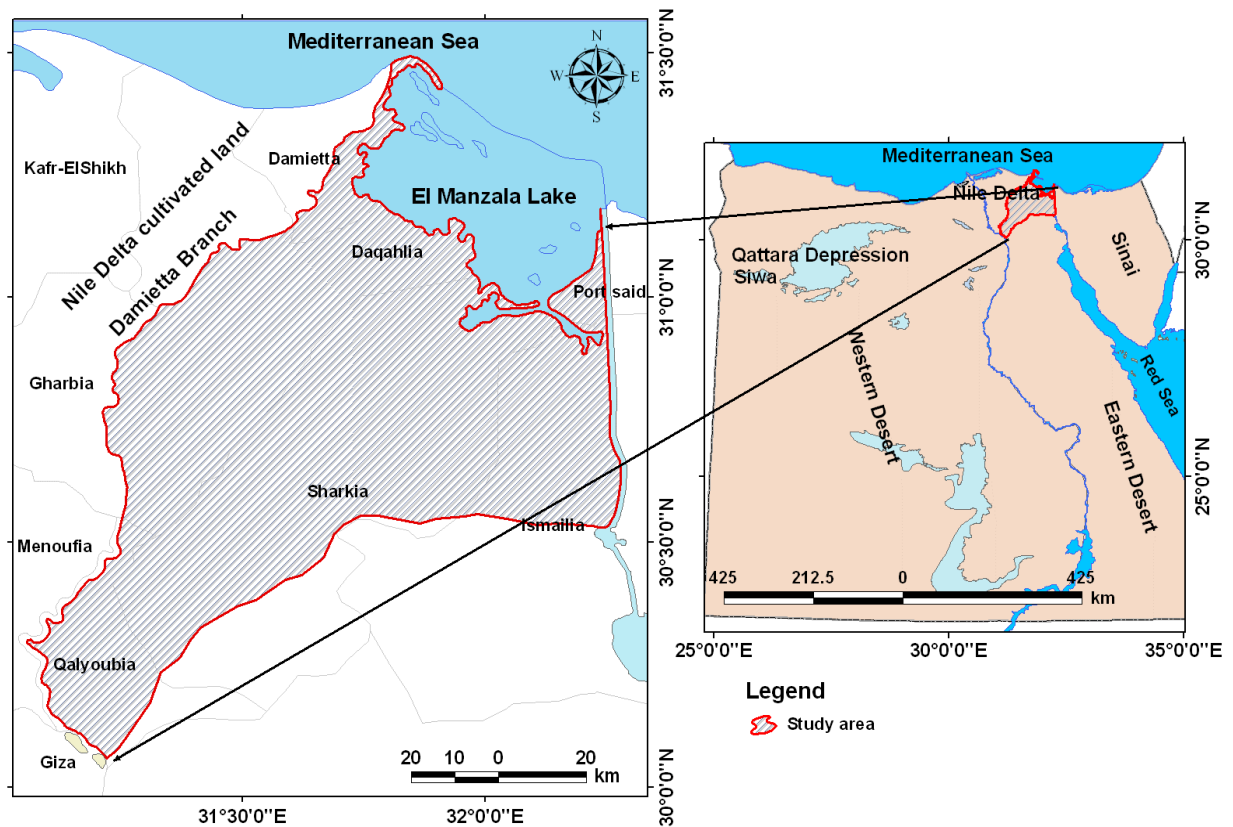
140

141 **2 Materials and Methods**

142 **2.1 Eastern Nile Delta Aquifer (Case Study Area)**

143 The Eastern Nile Delta aquifer was selected as a case study area to perform the numerical simulations. The
144 study area is bounded by the Damietta Branch at the West, El Manzala Lake at the North, Ismailia Canal at
145 the South and Suez Canal at the East, and its size is about 9500 km². It is located between latitudes 31° 00`
146 and 32° 30`N, and longitudes 29° 30` and 32° 30`E, as shown in Figure 1 (Nosair, 2011).

147 The aquifer system of the Nile Delta is one of the largest in the world for its areal extension and layer
148 thickness, with a total capacity of about 500 Bm³ (Sherif, 1999). Its characteristics have been identified by
149 numerous studies, assuming that it's formed by quaternary deposits and considered a semi-confined aquifer
150 as a whole (Al Agha, 2015). The geology of the aquifer includes Quaternary deposits of Holocene and
151 Pleistocene sediments, plus Tertiary deposits including the Pliocene, Miocene, Oligocene, Eocene, and
152 Paleocene sediments. The Quaternary aquifer thickness ranges from 100 m in the South, near Cairo, to
153 nearly 1,000 m at the coast of the Mediterranean Sea (RIGW, 1980). The hydrological strata are composed
154 of sands and gravels (Pleistocene and Holocene) containing few lenses of clays. These are considered the
155 main water-bearing formations (Sherif et al., 2012). The Quaternary base is a clay aquiclude with a slope
156 of about 4 m/km, which is about 40 times the ground surface slope (Serag EIDin, 1989; Said, 1993), as
157 shown in Figure 2. A number of studies were carried out on the Nile Delta aquifer system under different
158 scenarios of pumping rate (Sherif and Al-Rashed, 2001). In general, the most permeable layer has been
159 found at depths between 55 and 150 meters from the land surface (Sefelnasr and Sherif, 2014).



160

161

Figure 1: Location map of the East Nile Delta aquifer (from Nosair, 2011)

162

163

164

165

166

167

168

169

170

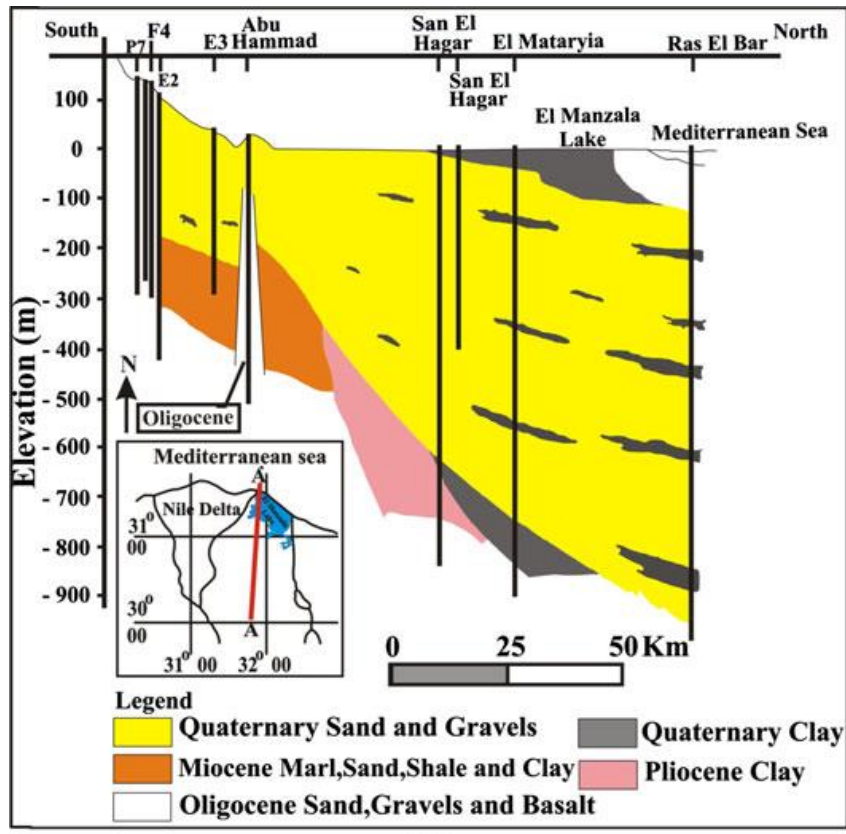
171

172

173

174

According to the field data compiled and processed by RIGW (1980), the top soil layer consists of clay, with a thickness that varies generally from 40 m in the North, middle and West Delta region, to about 90 m that are reached at the Damietta branch, with a general increment from West to East. So, according to the thickness of the clay layer, the semi-pervious clay cap admits leakage from the deepest to the shallow aquifer. The northern part of the aquifer is subject to upward flow, due to the difference in head of these water bodies that causes vertical movement of groundwater in the clay cap as shown in Figure 3. The quantity of upward flow in the delta aquifer is almost $50 \times 10^6 \text{ m}^3/\text{year}$ (Faried, 1979). On the other hand, the main aquifer is recharged by means of the irrigation canals, the seepage from the Damietta branch in Southwest and Ismailia Canal in the Southeast, plus the irrigation water excess. The latest estimates point out an amount of recharge deriving from irrigation practices of about 0.54 mm/day, while the average water loss by evaporation is around 311 mm/year (RIGW/IWACO 1990). According to different estimated depths of the groundwater table (reported by RIGW, 2002 and Morsy, 2009) the depth of the groundwater table in this aquifer ranges between 1- 2 m in the North, 3– 4 m in the center and 5 m in the South.

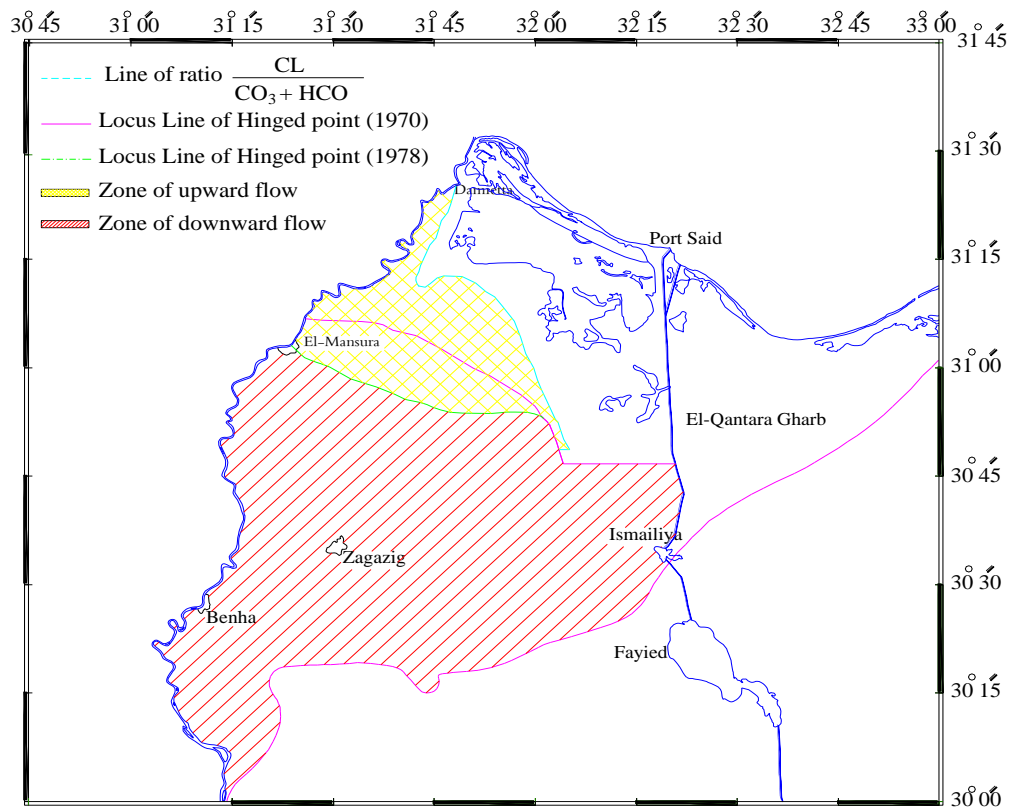


175

176

177

Figure 2: Longitudinal cross-section showing the thickness and litho-facies variation of the Quaternary aquifer in Nile Delta (from El Fayoumy, 1968)



178

179

180

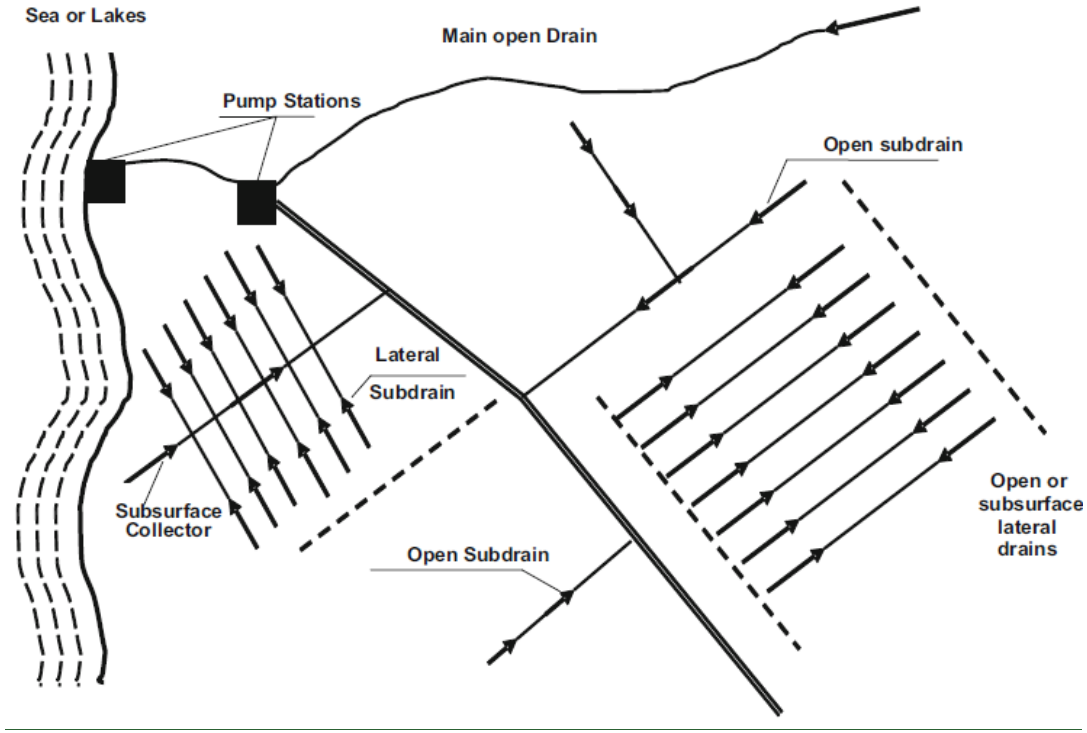
Figure 3: Locus line of the hinge points separating the upward and downward flow zones (After Amer, 1981)

181 Morsy (2009) estimated the total annual groundwater abstraction in the Nile Delta area to be 4.9 Bm³ in
182 2008, for irrigation and drinking purposes. The abstraction rate increases linearly by about 0.1 BM³ per
183 year, except the period from 2003 till 2010 by rate of 0.2 BM³ per year (Sallam, 2018). In the study area of
184 this paper (the eastern Delta) the amount of groundwater used in agriculture is about 326 Mm³/year (Abu-
185 Zeid, 1991) while the total amount reached 1.38 Bm³ in 2008. The main contributions to groundwater
186 discharge are represented by subsurface drainage and overexploitation of the aquifer. According to Fawzi
187 & Kamel (1994), the groundwater is discharged into the drainage system at a rate of 1.0 mm/day in all the
188 northern (coastal) part of the Nile delta.

190 In 1979, Atta analyzed the salinity of groundwater in the Nile delta based on the sampling of 50 wells,
191 finding values between 227 ppm and 15264 ppm. The salinity generally increases towards the northeastern
192 zone, while the northern parts and the areas adjacent to the Nile River canals have lower salinity. Farid
193 (1980, 1985) presented maps of salinity distribution, where iso-salinity lines in terms of total dissolved salts
194 (TDS) range from 640 to 45,000 ppm, and vertical cross sections with iso-salinity lines (TDS) ranging from
195 1,000 ppm to 35,000 ppm. These results agreed with (Atta, 1979) and indicated that the northern zone is
196 highly saline due to saltwater intrusion. Morsy (2009) analyzed and presented the groundwater salinity
197 from 1960 to 2008 based on historical groundwater quality data taken from the literature and from the
198 Research Institute for Groundwater of the Egyptian National Water Research Center (RIGW) database for
199 wells at depths from 30 to 135 m. These analyses confirmed the results shown by Sakr et al. (2004), i.e.,
200 the depths at which higher groundwater salinity was found confirm the existence of a clay layer with low
201 permeability over the deepest confined aquifer. Such clay cap is above the depths where Laeven (1991)
202 found the intrusion of saline water. Interestingly, Sherif et al. (2012), Abd-Elaty et al. (2014) and Abd-
203 Elhamid et al. (2016) simulated and described that the seawater in the Nile aquifer migrated to a distance
204 range from 48 to 76.25 km and from 72.50 to 93.75 km from the shoreline for the iso-salinity lines (TDS)
205 at 35000 ppm and 1000 ppm, respectively.

206 The surface water network (Nile branches, drains and irrigation canals) has a fundamental function to
207 determine the hydrogeological conditions in the northern part of the East Nile Delta area. The subsurface
208 drainage system protects the irrigated soils against salt accumulation and enables recycling of the irrigation

209 water. It consists of an extensive drainage network of field drains, sub-collectors, collectors and main drains
 210 (Figure 4), which either convey the drainage water back to the Nile, or discharge into coastal or inland lakes
 211 or directly to the sea (MWRI, 2013).



212
 213 Figure 4: Schematic diagram of Nile delta surface and subsurface drainage networks
 214

215 **2.2 Description of the Numerical Model**

216 The numerical model used to simulate the seawater intrusion in the Nile delta aquifer is based on the
 217 assumption of phreatic coastal aquifer subject to a top-down infiltration due to recharge (rainfall plus
 218 irrigation) and a bottom-up flow through a confined aquifer.

219 Seawater intrusion phenomenon is a miscible variable density process governed by the following coupled
 220 system of flow and transport equations:

221

$$\phi \frac{\partial \rho}{\partial t} - \nabla \cdot \left(\frac{\rho \mathbf{K}}{\mu} (\nabla p + \rho g \nabla z) \right) = 0$$

$$\phi \frac{\partial (\rho C)}{\partial t} + \nabla \cdot (\rho \mathbf{q} C) - \phi \nabla \cdot (\rho \mathbf{D} \nabla C) = 0$$

222 (1)

223 where \mathbf{K} is the hydraulic conductivity tensor; p is pressure; ϕ is porosity; ρ and μ respectively are fluid
224 density and viscosity; g is the gravitational constant; C is the solute (salt) concentration; $\mathbf{D} = (\phi d + \alpha_T |\mathbf{v}|) \mathbf{I}$
225 $+ (\alpha_L - \alpha_T) \mathbf{v} \mathbf{v}_T / |\mathbf{v}|$ is the hydrodynamic dispersion tensor and d diffusion coefficient; α_T and α_L respectively
226 are transverse and longitudinal dispersivity; $\mathbf{v} = \mathbf{q} / \phi$ is the fluid velocity, and the superscript T denotes
227 transpose. System (1) is closed by specifying a constitutive relationship, $\rho = \rho_f + \beta C$, where $\beta = (\rho_s - \rho_f) / C_s$,
228 ρ_s and ρ_f being salt and freshwater density respectively, and C_s the saltwater concentration.

229 2.2.1 *Regional scale numerical model: Seawater intrusion in the Nile delta aquifer*

230 [The latest version of SEAWAT \(Langevin et al., 2008\), a coupled version of MODFLOW and MT3DMS to](#)
231 [integrate the density-dependent flow and the solute transport equation, was used to simulate seawater](#)
232 [intrusion in the Nile delta aquifer at a regional scale.](#)

233 Subsurface flow and solute transport in the main aquifer was modelled by using 160 rows and 124 columns
234 of active cells, with a cell dimension of 1.0×1.0 km². The Nile Delta aquifer was divided into eleven layers.
235 The first layer represents the clay cap with depth varied between 20 m in the North to 50 m in the North.
236 The other layers, which represent the Quaternary aquifer, were divided into slices of equal thickness, until
237 an average depth of 200 m near Cairo to a depth of 1000 m at the coast line.

238 A constant head boundary condition was set equal to zero at the [northern](#) boundary along the shore line,
239 also at the [western](#) boundary a fixed head was imposed, between 16.15 m at the North and 0.25 m at North.
240 On the other hand, the domain is bounded to the South by the Ismailia canal, with a variable water level
241 between 16.15 m at its [westernmost](#) point and 7.00 m at its [easternmost](#) point, so a Dirichlet boundary
242 condition was assigned. The East boundary was considered impermeable and a no-flow (Neumann)
243 boundary condition was set. During the simulation, the hydraulic head boundaries along the Nile branches
244 were assumed as constant. The hydrodynamic parameters fed to the model are shown in Table 1.

245

246

247 **Table 1:** Summary of hydraulic parameters used as an input to the model

Hydraulic Parameters	Value
Vertical Quaternary hydraulic conductivity K_v (m/d)	0.50 - 10
Horizontal Quaternary hydraulic conductivity K_h (m/d)	5 - 100
Vertical clay cap hydraulic conductivity K_v (m/d)	0.01 - 0.025
Horizontal clay cap hydraulic conductivity K_h (m/d)	0.10 - 0.25
Porosity	<u>0.25 - 0.40</u>
Longitudinal dispersivity (α_L) (m)	250
Transversal dispersivity (α_T) (m)	25
Diffusion coefficient (d) (m^2/day)	10^{-4}
Hydraulic Forcing	Value
Recharge (mm/day)	0.25 - 0.80
Total abstraction ($m^3/year$)	2.78×10^9

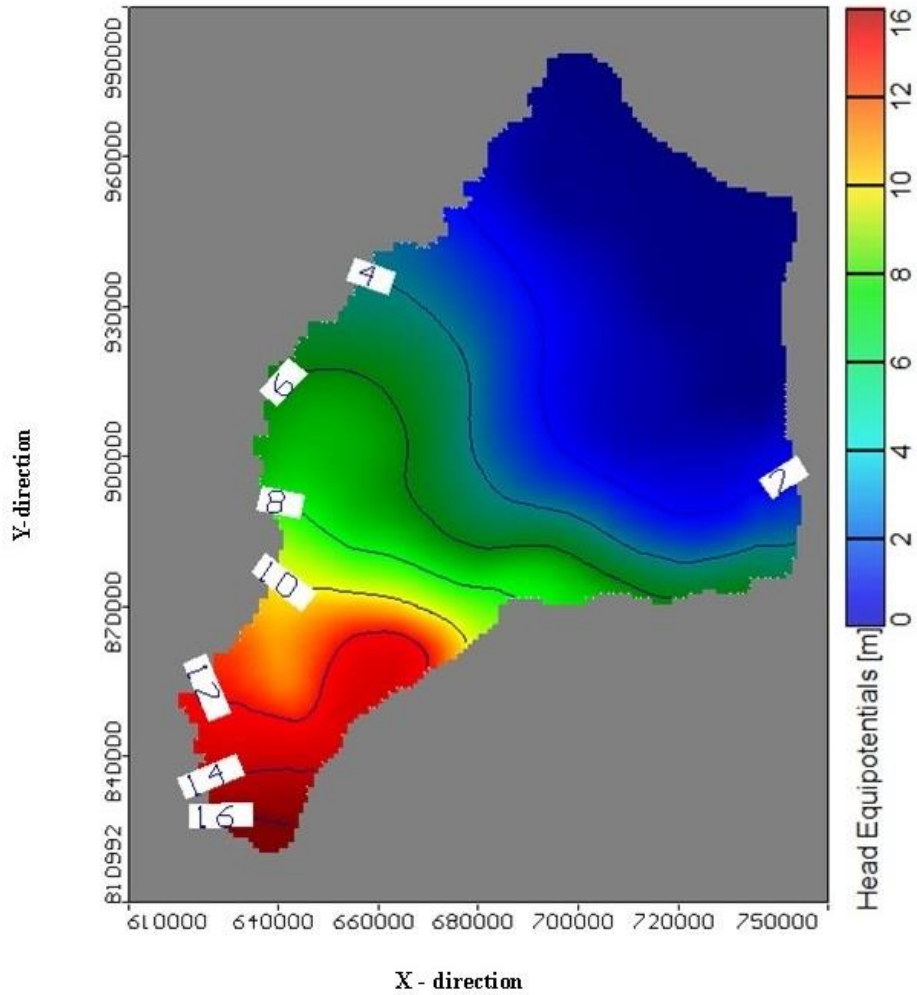
248

249 In order to obtain realistic results, the numerical model of the Nile Delta aquifer was calibrated by using
 250 available historical records, consisting in hydraulic head measurements in a number of piezometers
 251 distributed in the studied area, during a field campaign in 2008 (RIGW). The calibration of the numerical
 252 model was based on the comparison between modeled and measured hydraulic heads, by modifying the
 253 values of hydraulic conductivity, of porosity and of aquifer recharge rate, in order to optimize the match
 254 between the modeled and observed heads.

255 After calibration of the model, the maximum difference between measured and modeled heads (ranging
 256 from 16.00 to 0.0 respectively), is about 10 %, corresponding to about 1.60 m in the southernmost point.
 257 Comparing the calculated heads with the observed measurements in the Nile delta aquifer, the root mean
 258 square (RMS) of the residuals was equal to 0.329 m with a residual range between -0.215 and 0.488 m and
 259 a normalised RMS of 2.744 % (i.e. normalized with respect to the maximum difference in the observed
 260 head values). The results of the numerical model, in terms of hydraulic head (Figure 5), are in good
 261 agreement with the observed heads described in RIGW (2008).

262 A transport model has also been used to determine sea water intrusion (SWI) in the Eastern Nile delta
 263 aquifer. Firstly, it was calibrated by using field data of saltwater intrusion published by Sherif et al. (2012).
 264 The hydrodispersive parameters (i.e. α_L and α_T) contained in equations (1) have been calibrated by
 265 comparing saltwater concentrations measured by Sherif et al. (2012) with modeled concentrations.
 266 Calibration results are presented in Figure 6, which shows the distribution of total dissolved salts (TDS) in
 267 the middle of the aquifer (layer #6), assigning an average thickness of 450 m at the North and 100 m at the

268 South. These values are in good agreement with the field data of SWI in the Nile delta aquifer by Sherif et
269 al (2012). The isochlorine at 35000 ppm reaches a distance of 75.85 km from the shoreline, while the
270 isochlorine at 1000 ppm reaches a distance of 90.40 km.



271

272

Figure 5: Map of calculated groundwater head (simulation model) in the studied aquifer

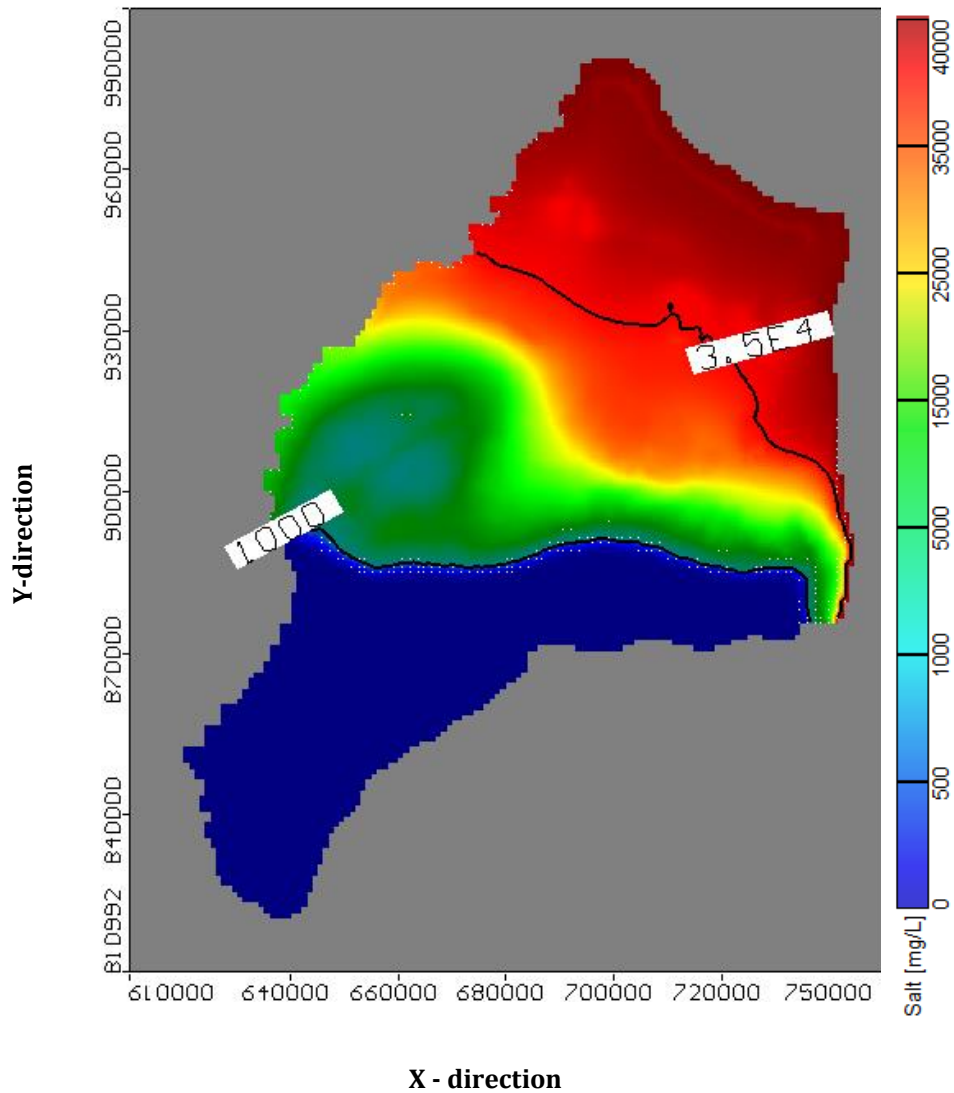


Figure 6: Map of TDS (output by SEAWAT) in the studied aquifer

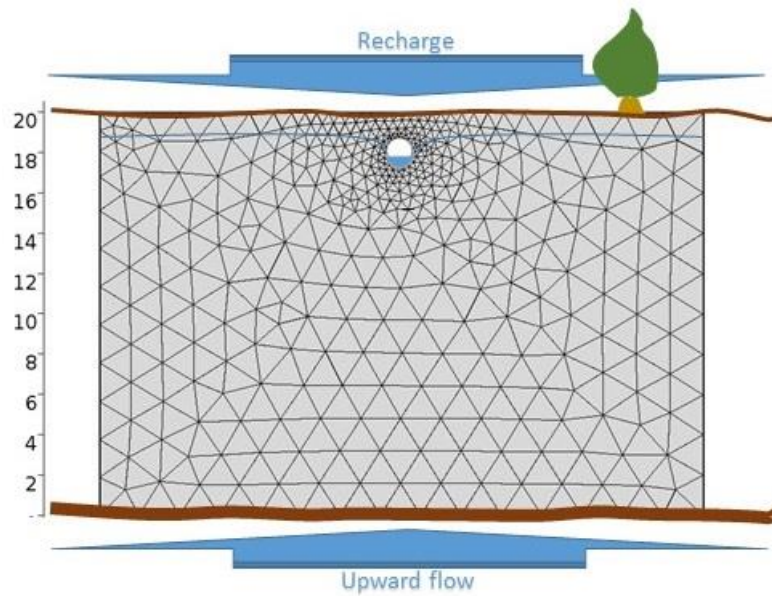
2.2.2 Local scale numerical model: subsurface drain discharge

In some areas of the Nile delta, especially in the North, the risk of water logging and salinisation due to the upward seepage from the underlying aquifer is very serious. Subsurface drainage systems, installed in the soil overlying artesian aquifers, offer a practical solution to the problem of upward artesian (brackish) water movement. The drain size and spacing need to be properly calculated (Abdel-Dayem, 1984) to make the drainage system able to discharge the excess of irrigation water as well as the upward groundwater flow. In practice, subsurface drains must be designed to withstand the necessary water flow, which permits to tie the water table to the required depth, for any foreseen working condition that may happen within the lifetime of the hydraulic structure. Thus, in the particular case of the Nile delta and of coastal aquifers in general,

284 the SD design must take into account the effects of SLR, subsidence, and all the human actions on the
285 groundwater flow (e.g. over-pumping, surface flow reduction, artificial recharge, etc.). This is a mandatory
286 effort to be done, in order to guarantee resilience of agricultural practices towards possible climate change
287 scenarios. It must be noted that this effort has been substantially underestimated until today.

288 The hypothesized geometry for the draining system considered in this study consists in a series of identical
289 parallel drains, regularly distributed with an equal spacing distance, orthogonal to a main collector.

290 A Finite Element Model was implemented in the COMSOL Environment (COMSOL, 2008) in order to
291 simulate the response of the subsurface drainage system to the actions of SLR, artificial recharge and
292 subsidence. The numerical model has a domain size of 20.0×30.0 m² discretized with 5000 irregular
293 elements (Figure 7). The main hydrological parameters used for the simulation of the drain system geometry
294 are the hydraulic conductivities ($K_h = 1.83 \times 10^{-6}$ m/s = $10 \times K_v$) and the porosity ($\phi = 0.3$). The main forcing
295 acting on the model is the hydraulic head variation ΔG (cm) observed at the drain level due to SLR, recharge
296 increment and subsidence.



297
298 Figure 7: Design criteria of the drainage system at an artesian aquifer
299

301 This model is used to calculate how the flow rate into the drains is modified by different working conditions,
302 linked to the said climate-related scenarios, for the fixed geometry (in particular, given the distance between
303 adjacent drains and their underground depth). By analyzing a set of possible future combinations of SLR,
304 subsidence and recharge within the next tens of years, useful estimations for an optimal performance of the
305 drainage system can be done.

2.3 SLR datasets

The estimation of SLR is carried out by analyzing the time series of tide gauge measurements (sometimes longer than 100 years), which are today completed by satellite radar altimetry measurements (about 25 years of global data at the time of writing this paper). The combination of advanced radar altimetry techniques, GPS and Synthetic Aperture Radar (SAR) interferometry with the persistent scatterer technique (Crosetto et al, 2016), permits to cross-validate such challenging measurements and separate the contributions of SLR and vertical land motion (VLM) to tide gauge measurements.

For what regards the mere SLR estimation on the coasts of the Nile delta, Essink and Kleef (1993) indicated 60 cm as a reasonable estimate within a time horizon of 100 years. The current estimation of the average global SLR derived from satellite altimetry is about 3.3 mm/year with an acceleration of 0.1 mm/y² (Legeais et al., 2018), and it's very variable on a geographical basis, as stated by the ESA Sea-Level CCI (Climate Change Initiative) project (ESA SL-CCI, 2018). Actually, one of the main issues of satellite radar altimetry lies in the extraction of accurate sea level estimations when approaching the coasts (Vignudelli et al., 2011). In the absence of a global coastal sea level product, near-shore measurements at the northern coasts of the Nile delta would require a specific study, which falls outside the scope of this paper. Instead, gridded data of global mean sea level (for open ocean studies) have already been produced by the altimetry community and can be used for rough estimates, provided that datapoints closest to the coasts are usually few km off the shoreline (the spatial resolution is 1/4 of degree). Based on the regional mean sea level trend map published by the CCI project, the SLR in front of the Nile delta coasts can be roughly estimated in 4 mm/year. A deeper discussion of SLR rate and acceleration, with an adequate approximation for the purpose of this paper, is provided in Section 3.1.

3 Results and Discussion

3.1 The effect of SLR and recharge on the coastal aquifer and its quantification

The objective of this section is to estimate the effects of a hypothetical future SLR on the piezometric head and its impact on the SD system [by means of the regional numerical model](#). All the following evaluations are made in terms of foreseen scenarios used to determine the hypothesized inputs to the numerical models.

333 Thus, hypotheses are done for a structure built in year 2000 (taken as a time reference), and scenarios are
334 calculated relating to years 2020, 2040 and 2060, in order to better understand the possible impact of such
335 phenomena within a time horizon compatible with the life expectancy of the buried draining structure..

336 SLR values for the three time horizons selected were determined according to the most recent available
337 information at the time of writing this paper. Being the fundamental aspects of SLR estimation already
338 introduced in Section 2, here we briefly discuss the reasoning behind the values fed as an input to the
339 modelling exercise.

340 A constant SLR rate has been assigned to the eastern shoreline of the Nile delta, by averaging selected grid
341 points from the sea-level CCI data base (ESA SL-CCI, 2018), which estimates mean sea level variations by
342 combining multiple satellite altimetry missions. By averaging the closest grid points to the interested
343 shoreline (7 points total) we obtained an SLR rate of 3.20 mm/yr. The cited SL-CCI data are referred to
344 year 2016, thus, cumulated mean sea level variations with respect to year 2000 (for the selected years 2020,
345 2040 and 2060) were calculated by introducing an additional acceleration to the said SLR rate. The most
346 updated global SLR acceleration rate is calculated in (Nerem et al., 2018), where the authors estimate a
347 “climate-change–driven” acceleration of 0.084 mm/y².

348 Based on these assumptions, SLR values of 5.7 cm, 14.5 cm and 26.7 cm (referred to year 2000) were
349 estimated for the years 2020, 2040 and 2060, respectively.

350 The results of the regional numerical model show an advancement of the sea water intrusion (SWI) in all
351 three cases. Specifically, the isochlorine at 35000 ppm reaches a distance from the shoreline of 76.25 km,
352 76.50 km and 77.05 km respectively (it was 75.85 km in year 2000), while the isochlorine 1000 ppm reaches
353 a distance of 90.60 km, 90.75 km and 90.85 km, respectively. These results confirm that SLR leads to
354 increase SWI in the whole aquifer with a southbound propagation, thus carrying an increased salinity of the
355 water and soil in the root zone, which is negatively impacting the crop productivity starting from the coastal
356 areas. The salt volume in the Eastern Nile Delta aquifer reaches 3.1288×10^{13} , 3.124937×10^{13} ,
357 3.123316×10^{13} , and 3.2116832×10^{13} Kg for a SLR of 0 cm, 5.7 cm, 14.5 cm and 26.7 cm, respectively. The
358 percentages of aquifer salt volume were increased by 1.50%, 2% and 4%, confirming that SLR leads to
359 increase the salt volume in the aquifer.

360 An artificial recharge scheme is thus hypothesized, in order to counteract the incremented SWI due to SLR.
 361 To do that, the approach followed in this research applies a recharge upstream the [Nile](#) delta (i.e., in its
 362 [northern](#) part) at variable percentage rates. This permits to foresee more complete and effective scenarios
 363 for the future design of subsurface draining systems and for the assessment of the draining systems that are
 364 currently active. A total of 9 runs of the [regional](#) model were carried out, in order to simulate all the
 365 combinations between SLR and the proposed recharge rates to control the SWI.
 366 Table [2](#) summarises the model results, taking into account both the expected SLR and 3 possible recharge
 367 scenarios, calculated in order to have an inversion of the intrusion process with the lowest value of recharge.
 368 The results in terms of intrusion length and aquifer salt volume (where C_0 is the initial salt concentration
 369 and C is the salt concentration at the given combination of SLR and recharge) are also shown in Table 3.

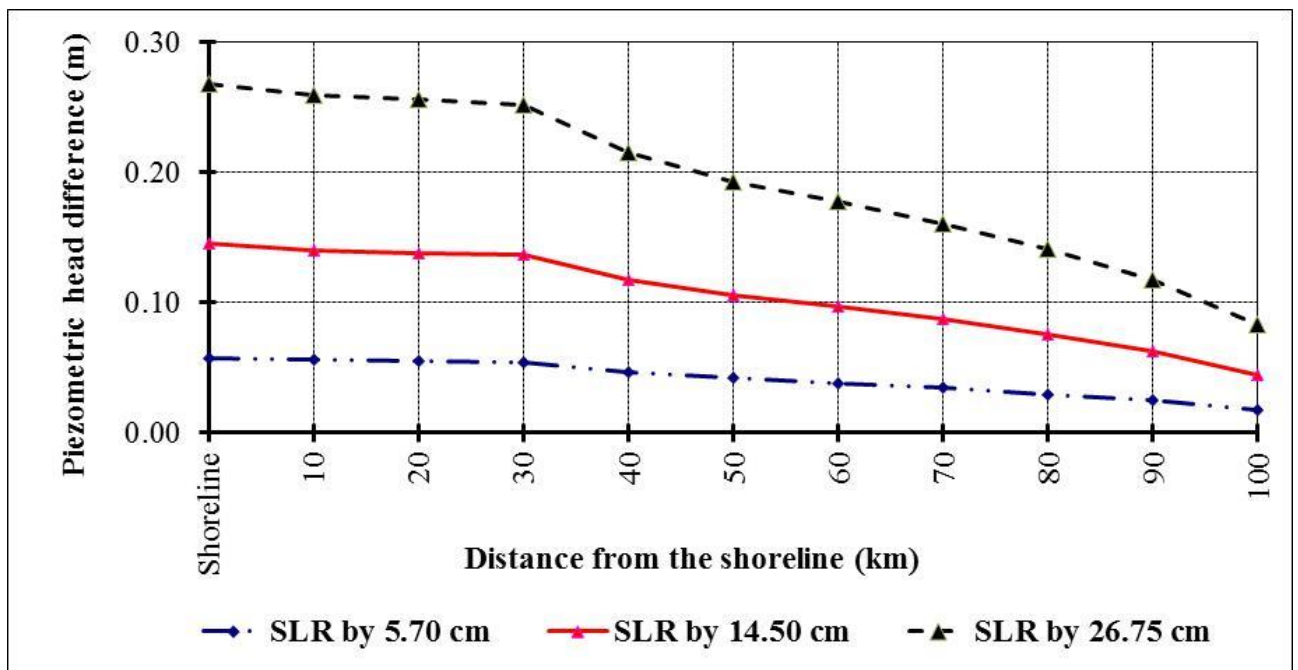
370 The table presents the percentage (%) of recharge required to keep the intrusion at the base case for three
 371 cases of SLR so the percentage of required recharge are 1, 1.50 and 3% at SLR of 5.70, 14.50 and 26.70
 372 cm while the intrusion reached 90.34, 90.36 and 90.34 for the isochlorine 1000 ppm while it reached 75.79,
 373 75.82 and 75.75 ppm for the isochlorine 35000 ppm. Also the aquifer salt variation $(C-C_0)/C_0$ were
 374 calculated to check the aquifer salt situation which the positive sign indicated that the aquifer salt is more
 375 than the base case and this is a negative impact to salt remove while the negative sign represents the recharge
 376 have a positive effect on saltwater intrusion.

377 **Table 2:** [Regional](#) model results as a function of SLR and various recharge levels

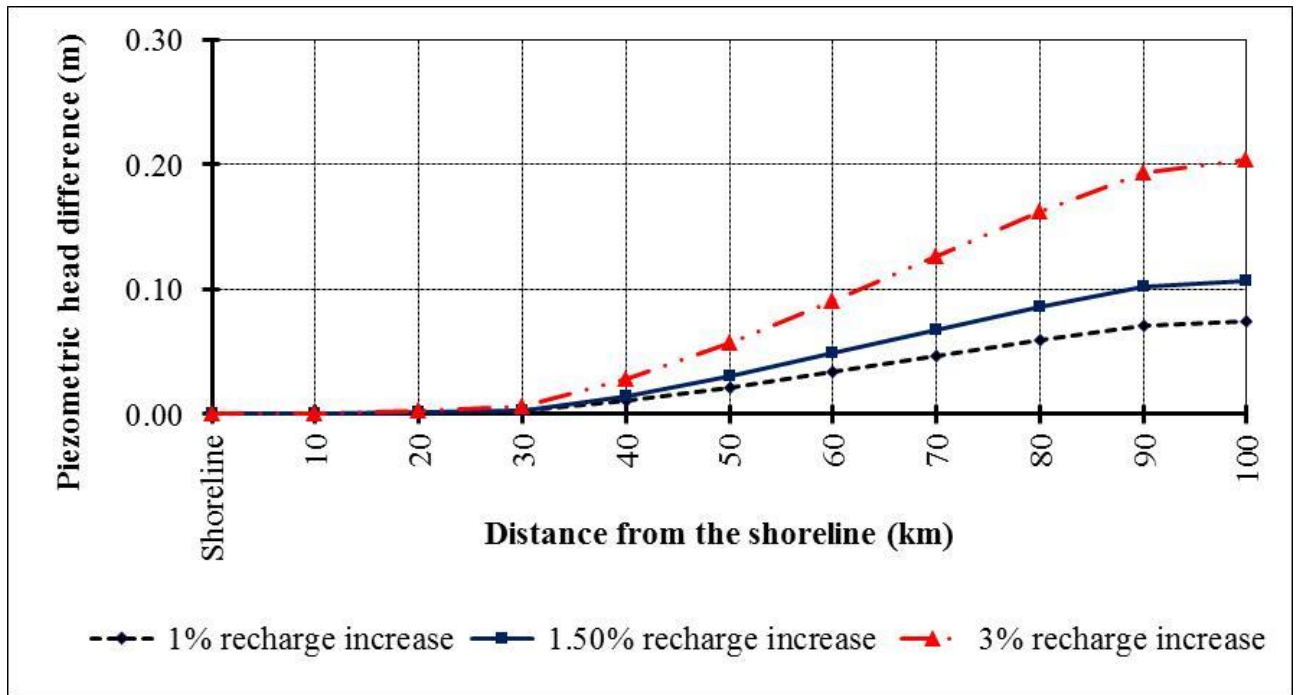
Time (year)	SLR (cm)	Recharge (%)	Intrusion length (km)		Aquifer salt variation $(C-C_0)/C_0$		Aquifer salt removal effect
			1000	35000	1000	35000	
2000	0	0	90.40	75.85	0	0	-
2020	5.7	0.50	90.37	75.87	+0.03	+0.02	negative
		1	90.34	75.79	-0.07	-0.08	positive
		1.50	90.30	75.72	-0.11	-0.17	positive
2040	14.5	1	90.39	75.90	-0.01	+0.06	negative
		1.50	90.36	75.82	-0.04	-0.03	positive
		2	90.33	75.75	-0.08	-0.13	positive
2060	26.7	2	90.4	75.90	0.00	+0.06	negative
		3	90.34	75.75	-0.07	-0.13	positive
		4	90.27	75.61	-0.14	-0.32	positive

378

379 It is clear that the three stages of SLR lead to increase [groundwater level](#) and SWI in the aquifer, as expected.
 380 This rising would damage a relevant quantity of freshwater in the aquifer, increasing the salinity of the soil
 381 and groundwater in the root zone.
 382 According to the model results, [the](#) control of SWI and soil salinity in the root zone under the hypothesized
 383 SLR conditions (5.7 cm, 14.5 cm and 26.7 cm) would be performed by artificially increasing the recharge
 384 by 1%, 1.5% and 3% respectively. This will lead to decrease SWI but increase [groundwater level](#). Figure 8
 385 shows the relationship between piezometric head difference and the distance from the shoreline under
 386 different SLR values and different scenarios of recharge. Figure 9 shows that the maximum difference in
 387 head occurs at the South, due to the maximum values of recharge applied there. The piezometric heads in
 388 the aquifer in the case study area under the different scenarios of recharge are shown in Table 3, which will
 389 be fully discussed later in this paper.



390
 391 Figure 8: Relation between piezometric head difference and distance from the shoreline for the proposed
 392 scenarios of SLR



393

394
395

Figure 9: Relation between piezometric head difference (G) and distance from the shoreline according to the three proposed scenarios of SLR and recharge

396

3.2 The effect of subsidence on the coastal aquifer and its quantification

397

It is clear how a proper design of subsurface draining systems contributes to mitigate the vulnerability to climate change and to the increased anthropic pressure. The main parameters that have been considered until now are the sea level rise and the increased seepage from recharge. In the particular case of the Nile delta, it is important to analyse also the effect of subsidence on the estimation of flow into the drains. The expected mechanism by which subsidence may affect the sizing of the drains consists in the reduction of distance between the semi-confined and the phreatic layers, due to compaction of the volume in between, and, consequently, the hydraulic head gradient between them.

404

An estimation of the current subsidence rates can be based on recent literature, where the vertical land motion in the Nile delta coasts is measured by SAR interferometric techniques, by using the “persistent scatterer” (PS) approach (Wöppelmann et al, 2013; Becker & Sultan, 2009). Few algorithms have been developed, in order to extract the Line Of Sight (LOS) deformation from SARIn data, and subsequently the vertical component of such deformation. To probe deeper into this technology, the interested reader may find relevant examples of said techniques in (Ferretti et al. 2001, Berardino et al. 2002, Hooper et al. 2004).

405

406

407

408

409

410 Recent estimates of subsidence rates in the Nile delta are provided by Fugate (2014), very useful for the
411 purpose of this paper even if mostly focused on the northwestern part of the delta. The work by
412 Wöppelmann et al (2013) combined the InSAR acquisition with GPS measurements, with an interesting
413 discussion of their relevant geodetic findings. The authors observed a very low rate of subsidence (about
414 0.5 mm/yr) in the Alexandria coastal region, with a good agreement between InSAR PS technique and the
415 tide gauge station in Alexandria. According to the authors, higher rates of about 5 mm/yr were observed in
416 the northeastern part of the Nile delta. Becker and Sultan (2009) found subsidence rates up to 8 mm/yr in
417 the northeastern coastal region, with relatively lower rates (4 to 6 mm/yr) around the Manzala lagoon.
418 Fugate (2014) substantially confirmed these velocities, finding subsidence rates around 8 mm/yr with
419 maximums about 10 mm/yr, in an area that covers a substantial part of the study area of this paper (Eastern
420 Nile delta aquifer).

421 All authors observed high spatial variability of ground motion velocities, characterized by a very irregular
422 spatial distribution, also in the presence of both uplift and subsidence phenomena in nearby zones. Despite
423 that, a general trend to higher subsidence rates is clearly asserted for what regards the northeastern coastal
424 region, with respect to the central and western ones. It is also important to underline here that the next
425 filling of the GERD is expected to negatively affect vertical land motion velocities in the Nile delta, due to
426 the lower water levels that will be experienced in the canals during the filling period and its possible direct
427 geotechnical implication.

428 For the purpose of this paper, we assigned a constant subsidence rate of 8 mm/yr to the whole study area,
429 as a cautious value to understand and better define the possible scenarios and their impact on the design of
430 the drainage infrastructure. Table 3 in the next section shows the incremental contribution of subsidence to
431 the flow into the SD system, combined with the other influencing factors (SLR and total recharge).

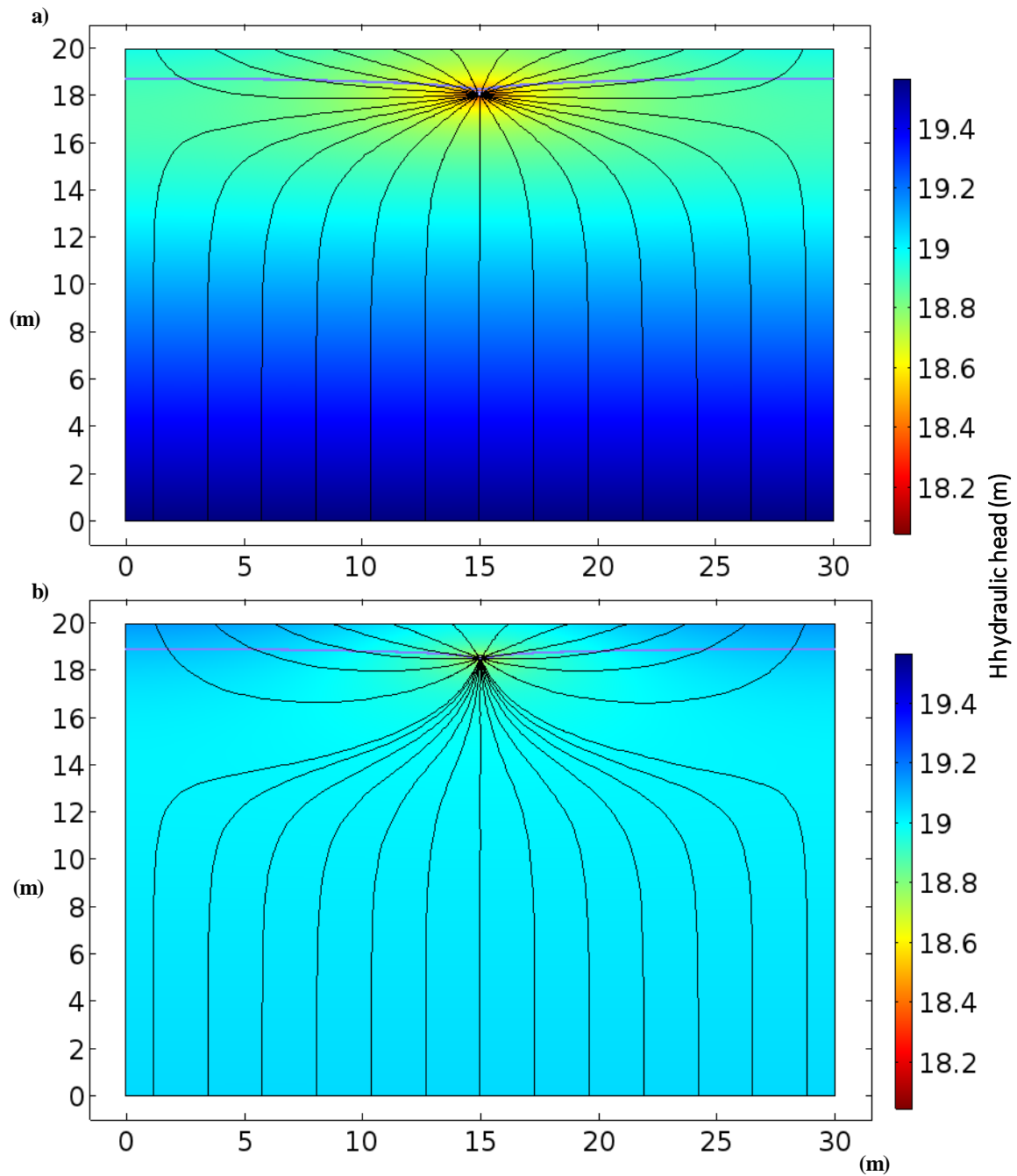
432 **3.3 Quantification of the impact on the subsurface drainage system design**

433 The previous sections demonstrated that the maximum increase of the piezometric head due to SLR occurs
434 in the northern part of the study area, where the aquifer is directly connected with the sea. Also salinity
435 experiences its maximum increase due to SLR on the northern coast, gradually decreasing toward the South.

436 Given this spatial trend, Table 3 shows the values of the predicted piezometric heads (ΔG), calculated at a
437 predetermined distance to the shore line (about 40 km) within the study area.

438 Given the foreseen increase of the piezometric heads, the impact of the increase of the piezometric heads
439 (ΔG) on the SD performance could be calculated by using [local scale numerical model described in section](#)
440 [2.2.2](#). More specifically, the subsurface drain discharge was calculated towards the predicted piezometric
441 heads according to the different stressors, separately: i) SLR; ii) recharge increment and iii) subsidence.
442 This has been done in order to make clear to the reader the importance of each contribution.

443 Figure 10 illustrates the hydraulic head distribution around the drains [obtained with local numerical model](#),
444 in the aquitard and in the phreatic aquifer in the given conditions. Table 3 summarises the simulation results
445 for the proposed scenarios. In particular, the table shows the incremental contributions of SLR, recharge
446 and subsidence to the flow into the SD system (named Q_{SLR} , Q_R and Q_{Sub} , respectively). SLR values of 5.7
447 cm, 14.5 cm and 23.75 cm were respectively assigned to the years 2020, 2040 and 2060, and entered in the
448 numerical model (based on Eq. 1). [As a consequence, piezometric heads due to SLR \(\$\Delta G_{SLR}\$ \) are](#)
449 [calculated in 4.65, 11.70 and 21.50 cm, respectively](#). The estimated increment of discharge Q_{SLR}
450 resulted about 0.81, 2.05 and 3.76 L/day·m for the three consecutive time horizons.



451 Figure 10: Water table (blue line), hydraulic head (false colors) and flow lines (black lines) around a
 452 drain. a) Scenario without SLR, Recharge and Subsidence (related to year 2000). b) Worst scenario with
 453 the maximum SLR, Recharge and Subsidence (year 2060).
 454

455

456 When an increment of recharge is hypothesized towards increasing sea level scenarios, the discharge
 457 through the drains also increases, with an impact on the efficiency of the SD system that must be taken into
 458 account. Thus, further calculations of the model have been performed, inclusive of the additional input due
 459 to recharge, as described in Section 3.1. The increment of discharge Q_R through the SD system has been
 460 calculated in about 0.19, 0.26 and 0.49 L/day·m, corresponding to 1%, 1.5% and 3% of recharge, which, in

turn, increased the piezometric heads due to recharge (ΔG_R) to reach 1.10, 1.50 and 2.80 cm respectively (Table 3).

Finally, the role of subsidence has been quantified. In particular, the reduction of the distance (in terms of depth below the soil level) between the SD and the hydraulic head was considered as a further input to the model. As a result, additional discharge increments of 2.73, 5.74 and 8.69 L/day·m, corresponding to the subsidence values assigned to the years 2020, 2040 and 2060, were obtained.

Considering all the inputs, the numerical findings show a total discharge increment of about 12.50%, 26.97% and 43.35% with respect to the initial Q. Thus, the inclusion of the scenarios studied in this paper in a wider context of water resources management impacts the design of SD systems in a non-negligible way, clearly indicated by the increasing discharge rates to be governed. This result is very relevant for the water management of Nile delta area. In fact, the combination of multiple forcing parameters, such as SLR, artificial subsurface recharge (made to reduce the aquifer salinity) and subsidence require a pre-emptive action in the design and sizing of such fundamental hydraulic structures for the resiliency of agriculture in the area under study.

Table 3: Summary of simulation results for the proposed scenarios. The impact on SD flow increment is highlighted in bold

Time (year)	2000	2020	2040	2060
Seal level rise (cm)	0	5.7	14.5	26.7
ΔG_{SLR} (cm)	0	4.65	11.70	21.50
Q_{SLR} (L/day/m)	0	0.81	2.05	3.76
Recharge (%)	0	1	1.5	3
ΔG_R (cm)	0	1.10	1.50	2.80
Q_R (L/day/m)	0	0.19	0.26	0.49
Δ Subsidence	0	16	32	48
Q_{Sub} (L/day/m)	0	2.73	5.74	8.69
Q_{Total} (L/day/m)	29.84	3.73	8.05	12.94
<u>Variation of Q (%)</u>	0	12.50	26.97	43.35

4 Conclusions

In this paper, the effect of climate-related drivers on the design of subsurface drainage systems in coastal aquifers is analysed by estimating the flow rate in the draining pipes and its possible increment due to hypothesized conditions of sea level rise, recharge and subsidence. Both surface and subsurface drainage networks in the northern part of the East Nile Delta were designed and realized in the past years, offering an exemplary study area for this research. The evaluations made in this paper are in terms of foreseen scenarios within a time horizon compatible with the life expectancy of the buried draining structure, taking year 2000 as a starting point and years 2020, 2040 and 2060 as reference years for the modelling exercise.

Regarding the climate change effects, the forcing parameters and their assigned values are briefly listed as follows:

- i. Based on a “climate-change–driven” acceleration of 0.084 mm/yr^2 , sea level rise values of 5.7 cm, 14.5 cm and 26.7 cm (referred to year 2000) were estimated for the years 2020, 2040 and 2060, respectively;
- ii. An increment of artificial recharge in order to counteract the incremented sea water intrusion (thus, soil salinity in the root zone) is needed. The hypothesized sea level rise values (5.7 cm, 14.5 cm and 26.7 cm) imply a recharge increment of about 1%, 1.5% and 3%, respectively;
- iii. According to recent literature data, subsidence values of 16 cm, 32 cm and 48 cm (referred to year 2000) were calculated for the years 2020, 2040 and 2060, respectively;

Regarding the climate change impacts on the subsurface drainage system (i.e. the increment of flow rate) the outcome of our analyses are:

- iv. For what regards the sea level rise, we estimated a discharge increment of about 0.81, 2.05 and 3.76 L/day/m , corresponding to 5.7 cm, 14.5 cm and 23.75 cm of SLR, respectively;
- v. For what regards the artificial recharge, a discharge increment of about 0.19, 0.26 and 0.49 L/day/m was evaluated, corresponding to 1%, 1.5% and 3% of recharge, respectively;
- vi. For what regards the subsidence, we estimated a discharge increment of about 2.73, 5.74 and 8.69 L/day/m , corresponding to subsidence values of 16, 32 and 48 cm, respectively;

504 vii. Considering all the forcings (i.e., sea level rise, artificial recharge and subsidence), the
505 numerical findings show a total discharge increment of about 3.73 L/day·m, 8.05 L/day·m and
506 12.94 L/day/m corresponding to a share of 12.50%, 26.97% and 43.35% with respect to the
507 initial flow rate (year 2000).

508 This result is very relevant to the future groundwater management in the Nile delta area. In fact, the
509 combination of multiple forcings, such as sea level rise, artificial subsurface recharge (for reducing the
510 aquifer salinity) and subsidence, imply the need for region-specific action plans to minimize the effects of
511 such stressors on the subsurface drainage system. In a wide context of water resources management, the
512 design of subsurface drainage systems must take into account the effects of climate change as a fundamental
513 component of the designing exercise. In particular, this paper demonstrates that the impact of the foreseen
514 conditions on the discharge into the subsurface drainage systems is anything but negligible.

515 **References**

- 516 [Abd-Elaty, I. M., Gehan.A.H.Sallam, Abdelaal, G. M., Eldin, O. W., \(2010\). Environmental Impact](#)
517 [Assessment of Subsurface Drainage Projects in Egypt, the Egyptian International Journal of Engineering](#)
518 [Science and Technology ,Vol. \(13\), No.\(2\), pp 411 – 418.](#)
519
- 520 Abd-Elaty, I. M., Abd-Elhamid H. F., Fahmy, M. R. and Abdelaal, G. M., (2014).” Investigation of some
521 Potential Parameters and its Impacts on Saltwater Intrusion in Nile Delta Aquifer”, Journal of Engineering
522 Sciences, Assiut University, Faculty of Engineering, Vol. (42), No. (4), PP 931-955.
523
- 524 Abdel-Dayem, M. S. Y., (1984). Drain Spacing for falling water table in a clay cap over an artesian aquifer,
525 PhD thesis, faculty of engineering, Cairo university, Egypt.
526
- 527 Abd-Elhamid H., Javadi A., Abd-Elaty I., and Sherif M. (2016). Simulation of seawater intrusion in the Nile
528 Delta aquifer under the conditions of climate change, Hydrology Research.
529
- 530 Abd-Elhamid H. and Abd-Elaty I. (2017). Application of a new methodology (TRAD) to control seawater
531 intrusion in the Nile delta aquifer, Egypt, Solutions to Water Challenges in MENA Region Proceedings of
532 the Regional Workshop, April 25-30, 2017 - Cairo, Egypt.
533
- 534 Abd-Elhamid H., Abd-Elaty I., & Sherif M. (2018). Evaluation of potential impact of Grand Ethiopian
535 Renaissance Dam on Seawater Intrusion in the Nile Delta Aquifer. International Journal of Environmental
536 Science and Technology, pp. 1-12.
537
- 538 Aboel Ghar M., Shalaby A. & Tateishi R. (2004). Agricultural land monitoring in the Egyptian Nile Delta
539 using Landsat data. International Journal of Environmental Studies, 61(6), 651-657, DOI:
540 10.1080/0020723042000253866.
541
- 542 [Abu-Zied, M., and Abdel-Dayem, G. \(1991\) Soil load in irrigation and drainage water in the Nile Delta, In:](#)
543 [African Regional Symposium on Techniques for environmentally sound water resources Development.](#)
544

545 Agren J., Svensson R. (2007). Postglacial Land Uplift Model and System Definition for the New Swedish
546 Height System RG 2000; Lantmäteriet: Gävle, Sweden.

547

548 Amer, A.M., (1981). Physics of the Nile Delta Aquifer. Proceedings of International Workshop on
549 Management of the Nile Delta Groundwater Aquifer, Cairo University, Giza, Egypt.

550

551 Atta A. S. (1979). Studies on the groundwater properties of the Nile Delta, Egypt, M.Sc. Thesis, Fac. of Sc.,
552 Cairo University, 311–325.

553

554 Bazaraa A. S., Abdel-Dayem M. S, Amer A., and Willardson L. S., (1986). Artesian and Anisotropic Effects
555 on Drain Spacing, Journal of Irrigation and Drainage Engineering, Vol. 112, No. 1, February 1986, pp.
556 55-64.

557

558 Becker, R. H., & Sultan, M. (2009). Land subsidence in the Nile Delta: inferences from radar interferometry.
559 The Holocene, 19(6), 949-954.

560

561 Berardino, P., Fornaro, G., Lanari, R., & Sansosti, E. (2002). A new algorithm for surface deformation
562 monitoring based on small baseline differential SAR interferograms. IEEE Transactions on Geoscience
563 and Remote Sensing, 40(11), 2375-2383.

564

565 British Columbia Agriculture & Food Climate Action Initiative (2013) BC Farm Practices & Climate Change
566 Adaptation series: Drainage, www.BCAGClimateAction.ca.

567

568 COMSOL Multiphysics (2008). User's guide version 3.5, Stockholm.

569

570 Crosetto M., Monserrat O., Cuevas-González M., Devanthéry N. & Crippa B. (2016). Persistent scatterer
571 interferometry: A review. ISPRS Journal of Photogrammetry and Remote Sensing, 115, 78-89.

572

573 Deelstra J. (2015) Climate change and subsurface drainage design: results from a small fieldscale catchment
574 in south-western Norway, Acta Agriculturae Scandinavica, Section B — Soil & Plant Science, 65:sup1,
575 58-65, DOI: 10.1080/09064710.2014.975836

576

577 EI-Fayoumi, F., (1987). Geology of the Quaternary Succession and Its Impact on the Groundwater Reservoir
578 in the Nile Delta Region, Bull. Fac. Sci., Menofia Univ., Egypt.

579

580 El Raey M., (2010) Impact and Implications of Climate Change for the Coastal Zones of Egypt. In: Michel,
581 D., Pandya, A. (eds.) (2010), Coastal Zones and Climate Change.

582

583 ESA SL-CCI (2018) <http://www.esa-sealevel-cci.org/node/248>, accessed 19 June 2018.

584

585 Essink K. and Kleef H. L.(1993). Distribution and life cycle of the North American spionid polychaete
586 Marenzelleria viridis (verrill,1873) in the Ems estuary, edited by: Meire, P. and Vincx, M., 1993.

587

588 Fawzi I., Kamel M.S. (1994). Design of drainage system, design criteria adopted by EPADP. Refreshing course
589 on land drainage in Egypt, 10-19 December 1994.

590

591 Faried M. S., (1979). Nile delttta groundwaer study, unpublished M. Sc. thesis, Faculty of Engineering, Cairo
592 University, Giza, Egypt.

593

594 Farid M.S.M. (1980) Nile Delta Groundwater Study, M.Sc. Thesis, Cairo University.

595

596 Farid M.S.M. (1985) Management of groundwater systems in the Nile Delta. PhD Thesis, Cairo Univ., Giza,
597 Egypt.

598
599 Ferretti A., Prati C., & Rocca F. (2001). Permanent scatterers in SAR interferometry. IEEE Transactions on
600 geoscience and remote sensing, 39(1), 8-20.
601
602 Fugate J. M. (2014). Measurements of land subsidence rates on the northwestern portion of the Nile Delta
603 using radar interferometry techniques (M. Sc. Thesis).
604
605 Hooper A., Zebker H., Segall P., & Kampes B. (2004). A new method for measuring deformation on volcanoes
606 and other natural terrains using InSAR persistent scatterers. Geophysical research letters, 31(23).
607
608 IPCC (2008). Climate Change and Water, Technical Paper of the Intergovernmental Panel on Climate Change,
609 edited by: Bates, B. C., Kundzewicz, Z. W., Wu, S., and Palutikof, J. P., IPCC Secretariat, Geneva, p.
610 210.
611
612 IPCC (2013): Climate Change 2013: The Physical Science Basis. Contribution of Working Group I to the Fifth
613 Assessment Report of the Intergovernmental Panel on Climate Change [Stocker, T.F., D. Qin, G.-K.
614 Plattner, M. Tignor, S.K. Allen, J. Boschung, A. Nauels, Y. Xia, V. Bex and P.M. Midgley (eds.)].
615 Cambridge University Press, Cambridge, United Kingdom and New York, NY, USA, 1535 pp.
616
617 Kalantari Z. (2011). Adaptation of Road Drainage Structures to Climate Change, TRITA LWR LIC 2061
618
619 Langevin C.D., Thorne D.T. Jr., Dausman A.M., Sukop M.C., and Guo Weixing (2008). SEAWAT Version
620 4: A computer program for simulation of multi-species solute and heat transport: U.S. Geological Survey
621 Techniques and Methods, book 6, chap. A22, 39 p.
622
623 Laeven M.T. (1991). Hydrogeological study of the Nile Delta and adjacent desert areas, Egypt, with emphasis
624 on hydrochemistry and isotope hydrology, M.Sc. thesis, Free University, Amsterdam. Also published by
625 RIGW/IWACO as Technical Note TN 77.01300-91-01.
626
627 Legeais J.-F., Ablain M., Zawadzki L., Zuo H., Johannessen J. A., Scharffenberg M. G., Fenoglio-Marc L.,
628 Fernandes M. J., Andersen O. B., Rudenko S., Cipollini P., Quartly G. D., Passaro M., Cazenave A., and
629 Benveniste J. (2018). An improved and homogeneous altimeter sea level record from the ESA Climate
630 Change Initiative, Earth Syst. Sci. Data, 10, 281-301, <https://doi.org/10.5194/essd-10-281-2018>.
631
632 Morsy W. S. (2009). Environmental management to groundwater resources for Nile delta Region, PhD thesis,
633 Faculty of Engineering, Cairo University, Egypt.
634
635 Nerem R. S., Beckley B. D., Fasullo J. T., Hamlington B. D., Masters D., & Mitchum G. T. (2018). Climate-
636 change-driven accelerated sea-level rise detected in the altimeter era. Proceedings of the National
637 Academy of Sciences, 201717312, doi:10.1073/pnas.1717312115.
638
639 Nosair A. M. (2011). Climate changes and their impacts on groundwater occurrence in the northern part of
640 East Nile delta, M.Sc. Thesis, Faculty of Science, Zagazig University, Egypt.
641
642 MWRI (2013). Proposed climate change adaptation strategy for the Ministry of Water Resources and Irrigation
643 (MWRI) in Egypt, tech. report, Ministry of Water Resources and Irrigation, Egypt.
644
645 Pease L.A., Fausey N.R., Martin J.F., and Brown L.C.(2017). Projected climate change effects on subsurface
646 drainage and the performance of controlled drainage in the Western Lake Erie Basin, Journal of Soil and
647 Water Conservation, Vol. (72), No. 3.
648

- 649 RIGW/IWACO (1990). Development and management of groundwater resources in the Nile Valley and Delta:
650 Assessment of groundwater pollution from agricultural activities, Internal report, Research Institute for
651 Groundwater, El Kanater El Khairia, Egypt.
652
- 653 RIGW (Research Institute for Groundwater) (1980) Projected of the Safe Yield Study for Groundwater Aquifer
654 in the Nile Delta and Upper Egypt, part 1 (in Arabic). Ministry of Irrigation, Academy of Scientific
655 Research and Technology, and Organization of Atomic Energy, Egypt.
656
- 657 RIGW (2002). Nile Delta Groundwater Modeling Report. Research Inst. for Groundwater, Kanater El-Khairia,
658 Egypt.
659
- 660 [Said, R. \(1962\) The Geology of Egypt. Elsevier Publishing Company, Amsterdam, New York, 377 pp.](#)
661
- 662 [Said, R. \(1981\).The Geological Evolution of the River Nile. Springer-Verlag, New York, 151 pp.](#)
663
- 664 [Said, R., \(1993\). The Nile River: Geology, Hydrology, and Utilization. Pergamon, New York, USA, 320 pp.](#)
665
- 666 [Sakr S. A., Attia F. A., and Millette J. A. \(2004\). Vulnerability of the Nile Delta aquifer of Egypt to seawater
667 intrusion, International conference on water resources of arid and semi-arid regions of Africa, Issues and
668 challenges, Gaborone, Botswana.](#)
669
- 670 [Sallam O., M., \(2018\) Vision for Future Management of Groundwater in the Nile Delta of Egypt After
671 Construction of the Ethiopian Dams, Hydrology: Current Research, Vol \(9\), Issue \(3\).](#)
672
- 673 [Serag El-Din, H., 1989. Geological, Hydrogeological and Hydrological Studies on the Quaternary Aquifer,
674 Egypt, PhD Dissertation, Mansoura Univ., Egypt.](#)
675
- 676 Sestini G.(1989). Nile Delta: A review of depositional environments and geological history.
677 In Whateley, M.K.G. and Pickering, K.T. eds. : Deltas : Sites and Traps for Fossil Fuels. Geol.
678 Soc. Spec. Publ., 41, 99-127.
679
- 680 Shaltout M., Tonbol K., and Omstedt A. (2015). Sea-level change and projected future flooding along the
681 Egyptian Mediterranean coast, Oceanologia, v. 57, p. 293–307, doi: 10.1016/ j.oceano.2015.06.004.
682
- 683 Sherif M. M and Al-Rashed M. F. (2001). Vertical and Horizontal Simulation of Seawater Intrusion in the Nile
684 Delta Aquifer, Proceeding of the 1st International Conference and Workshop on Saltwater Intrusion and
685 Coastal Aquifers,Monitoring, Modelling, and Management (Morocco).
686
- 687 Sherif M.M., Sefelnasr A., and Javadi A. (2012). Incorporating the concept of equivalent freshwater head in
688 successive horizontal simulations of seawater intrusion in the Nile Delta Aquifer, Egypt. Journal of
689 Hydrology 464–465: 186–198. DOI: org/10.1016/ j.jhydrol.2012.07.007.
690
- 691 Sefelnasr. A. and Sherif M., (2014). Impacts of Seawater Rise on Seawater Intrusion in the Nile Delta Aquifer,
692 Egypt, Groundwater Journal, Vol. (52), No.(2), p. 264–276.
693
- 694 [Stanley, J.-D., and Corwin, K. A. \(2012\) Measuring Strata Thicknesses in Cores to Assess Recent Sediment
695 Compaction and Subsidence of Egypt's Nile Delta Coastal Margin: Journal of Coastal Research](#)
696
- 697 Vignudelli S., Kostianoy A.G., Cipollini P., Benveniste J. (Eds) (2011). Coastal Altimetry, Springer-Verlag
698 Berlin Heidelberg, pp. 19-50, doi:10.1007/978-3-642-12796-0_19
699

700 Wöppelmann G., Le Cozannet G., De Michele M., Raucoules D., Cazenave A., Garcin M., ... & Santamaría-
701 Gómez A. (2013). Is land subsidence increasing the exposure to sea level rise in Alexandria, Egypt?
702 *Geophysical Research Letters*, 40(12), 2953-2957.